Chinese Journal of Natural Medicines

Curvularin derivatives from hydrothermal vent sediment fungus *Penicillium* sp. HL-50 guided by molecular networking and their anti-inflammatory activity

Chunxue Yu, Zixuan Xia, Zhipeng Xu, Xiyang Tang, Wenjuan Ding, Jihua Wei, Danmei Tian, Bin Wu, Jinshan Tang

Citation: Chunxue Yu, Zixuan Xia, Zhipeng Xu, Xiyang Tang, Wenjuan Ding, Jihua Wei, Danmei Tian, Bin Wu, Jinshan Tang, Curvularin derivatives from hydrothermal vent sediment fungus *Penicillium* sp. HL-50 guided by molecular networking and their anti-inflammatory activity, Chinese Journal of Natural Medicines, 2025, 23(1), 119-128. doi: 10.1016/S1875-5364(25)60803-X.

View online: https://doi.org/10.1016/S1875-5364(25)60803-X

Chinese Journal of Natural Medicines 23 (2025) 119-128

Contents lists available at ScienceDirect

Chinese Journal of Natural Medicines

journal homepage: www.cjnmcpu.com/

Original article

Curvularin derivatives from hydrothermal vent sediment fungus *Penicillium* sp. HL-50 guided by molecular networking and their anti-inflammatory activity

Chunxue Yu[a,Δ], Zixuan Xia[a,Δ], Zhipeng Xu[a], Xiyang Tang[a], Wenjuan Ding[b], Jihua Wei[c], Danmei Tian[a,*], Bin Wu[c,*], Jinshan Tang[a,*]

[a] *Institute of Traditional Chinese Medicine and Natural Products, College of Pharmacy/Guangdong Province Key Laboratory of Pharmacodynamic Constituents of Traditional Chinese Medicine and New Drug Research/International Cooperative Laboratory of Traditional Chinese Medicine Modernization and Innovative Drug Development of Ministry of Education (MOE) of China, Jinan University, Guangzhou 510632, China*

[b] *School of Traditional Chinese Materia Medica, Shenyang Pharmaceutical University, Shenyang 110016, China*

[c] *Ocean College, Zhejiang University, Zhoushan Campus, Zhoushan 316021, China*

ARTICLE INFO

Article history:
Received 22 January 2024
Revised 29 March 2024
Accepted 9 April 2024
Available online 20 January 2025

Keywords:
Penicillium sp. HL-50
Curvularin derivatives
Molecular networking
Anti-inflammatory activity

ABSTRACT

Guided by molecular networking, nine novel curvularin derivatives (**1**–**9**) and 16 known analogs (**10**–**25**) were isolated from the hydrothermal vent sediment fungus *Penicillium* sp. HL-50. Notably, compounds **5**–**7** represented a hybrid of curvularin and purine. The structures and absolute configurations of compounds **1**–**9** were elucidated *via* nuclear magnetic resonance (NMR) spectroscopy, X-ray diffraction, electronic circular dichroism (ECD) calculations, ^{13}C NMR calculation, modified Mosher's method, and chemical derivatization. Investigation of anti-inflammatory activities revealed that compounds **7**–**9**, **11**, **12**, **14**, **15**, and **18** exhibited significant suppressive effects against lipopolysaccharide (LPS)-induced nitric oxide (NO) production in murine macrophage RAW264.7 cells, with IC_{50} values ranging from 0.44 to 4.40 μmol·L^{-1}. Furthermore, these bioactive compounds were found to suppress the expression of inflammation-related proteins, including inducible NO synthase (iNOS), cyclooxygenase-2 (COX-2), NLR family pyrin domain-containing protein 3 (NLRP3), and nuclear factor kappa-B (NF-κB). Additional studies demonstrated that the novel compound **7** possessed potent anti-inflammatory activity by inhibiting the transcription of inflammation-related genes, downregulating the expression of inflammation-related proteins, and inhibiting the release of inflammatory cytokines, indicating its potential application in the treatment of inflammatory diseases.

1. Introduction

Curvularin, a member of the polyketide family, was initially isolated from the fungus *Curvularia* sp. [1]. In recent decades, numerous curvularin derivatives have been identified in various fungal species, including *Aspergillus* sp. [2], *Alternaria* sp. [3], and *Penicillium* sp. [4]. The core structure of curvularin derivatives typically consists of a benzene ring fused to a twelve-membered macrocyclic lactone, often featuring substituents such as methoxyl, hydroxyl, and sulfur-containing groups at the C-11 position of the skeleton [4-6]. Furthermore, curvularin derivatives with a benzene ring fused to a six-membered cyclic ether have been documented, although only four such naturally occurring compounds have been reported to date [7,8]. Pharmacological investigations of curvularin derivatives have primarily focused on their phytotoxicity [9], cell division inhibition [10], anti-inflammatory properties [11], antimicrobial activity [12], and cytotoxicity [4]. Recent studies have demonstrated that curvularin derivatives, particularly 10,11-dehydrocurvularin, exhibit potent anti-inflammatory activities by inhibiting NLR family pyrin domain-containing protein 3 (NLRP3) inflammasome activation [11] and nuclear factor kappa-B (NF-κB) signaling pathway, while also reducing the expressions of inducible nitric oxide (NO) synthase (iNOS) and cyclooxygenase-2 (COX-2) in lipopolysaccharide (LPS)-stimulated RAW264.7 macrophages [13].

Recently, tandem mass spectrometry (MS/MS)-based molecular networking has emerged as a powerful tool for rapidly identifying novel metabolites in complex mixtures [14, 15]. During our investigation of bioactive metabolites from marine-derived fungi, facilitated by MS/MS-based molecular networking, we discovered that *Penicillium* sp. HL-50, isolated from hydrothermal vent sediment, contained numerous curvularin derivatives, some of which were previously undocumented. Consequently, a targeted study of curvularin derivatives from the HL-50 culture was conducted, resulting in the isolation of nine new curvularin derivatives (**1**–**9**) and 16 known analogs (**10**–**25**). Notably, compounds **5**–**7** represent the first reported instances containing a

* Corresponding author.
E-mail addresses: danmeitianjnu@163.com (D. Tian); wubin@zju.edu.cn (B. Wu); gztangjinshan@126.com (J. Tang)
Δ These authors contributed equally to this work.

https://doi.org/10.1016/S1875-5364(25)60803-X

purine moiety. Additionally, we evaluated the anti-inflammatory potential of the isolated compounds by assessing their inhibitory effects on NO production and the expression levels of inflammation regulatory proteins stimulated by LPS in murine macrophage RAW264.7 cells.

2. Result and discussion

The strain *Penicillium* sp. HL-50 was cultivated in rice solid medium for 45 d, and the cultures were extracted with ethyl acetate (EtOAc) to obtain the crude extract. The crude extract was analyzed by ultra-performance liquid chromatography/quadrupole time-of-flight (UPLC/Q-TOF) MS, and subsequent molecular networking was constructed on the Global Natural Products Social (GNPS) platform. Polyketides (mainly curvularin derivatives), fatty acids, alkaloids, shikimates, phenylpropanoids, and dipeptides were predicted to exist in the crude extract (Fig. 1). Among these, four proposed curvularin derivatives, *S*-curvularin, (10*E*, 15*S*)-10,11-dehydrocurvularin, methoxycurvularin, and sumalarin C, attracted our attention. Analysis of their fragmentation behavior revealed similar characteristic fragment ions at *m/z* 195, 167, and 123, consistent with previous reports (Table S1)[16]. Additional putative curvularin derivatives, including several new analogs, were elucidated in the A and B clusters by comparing their fragmentation behaviors with those of the proposed four analogs (Fig. 1). Guided by the GNPS molecular networking, nine new curvularin derivatives (**1**–**9**) (Fig. 2), along with 16 known analogs (**10**–**25**), were isolated from the cultures of *Penicillium* sp. HL-50. The known compounds were identified as *S*-curvularin (**10**) [4], (10*E*,15*S*)-10,11-dehydrocurvularin (**11**) [5] (10*Z*,15*S*)-10,11-dehydrocurvularin (**12**) [5], *β*,*γ*-dehydrocurvularin (**13**) [3], 11*β*-methoxycurvularin (**14**) [5], 11*α*-methoxycurvularin (**15**) [5], 11*β*-hydroxy-curvularin (**16**) [6], 11*α*-hydroxy-curvularin (**17**) [6], sumalarin C (**18**) [4], sumalarin A (**19**) [4], curvularin-7-*O*-*β*-D-glucopyranoside (**20**) [4], *S*-dothiorelone P (**21**) [17], cytosporone M (**22**) [18], *ent*-curvulone A (**23**) [19], 10*S*,11*S*,15*S*,18*R*-cyclothiocurvularin B methyl ester (**24**) [20], and cyclosulfoxicurvularin (**25**) [20] by comparing their physical and chemical properties with those reported in previous studies.

Compound **1** was isolated as colorless crystals (in MeOH). Its molecular formula was determined to be $C_{16}H_{20}O_6$ by high-resolution electrospray ionization mass spectrometry (HR-ESI-MS) at *m/z* 309.1341 $[M + H]^+$ (Calcd. 309.1338), indicating seven degrees of unsaturation. The ^{1}H nuclear magnetic resonance (NMR) spectrum of **1** revealed the signals for two aromatic protons at δ_H 6.30 (1H, brs) and 6.21 (1H, brs), suggesting the presence of a 1,2,3,5-tetrasubstituted aromatic ring, two oxymethines at δ_H 4.32 (1H, m) and 3.58 (1H, m), and a methyl at δ_H 1.05 (3H, d, J = 6.0 Hz). The ^{13}C NMR, supported by heteronuclear single quantum coherence (HSQC) spectra, indicated the presence of 16 carbon resonances: two carbonyl groups at δ_C 173.4 and 191.2, six aromatic carbons at δ_C 164.0, 163.4, 140.0, 114.2, 112.0, and 101.5, two oxymethines at δ_C 76.8 and 65.6, five methylenes at δ_C 43.3, 41.5, 38.8, 34.2, and 20.8, and a methyl at δ_C 23.7. These spectroscopic features suggested that **1** possesses the same 3,4-dihydro-7-hydroxy-4-oxo-2*H*-L-benzopyran-5-acetic acid core skeleton as corynechromone F [7]. Furthermore, the spin system of H-10/H-11/H-12/H-13/H-14/H-15/H-16 observed in the ^{1}H-^{1}H correlation spectroscopy (COSY) indicated the presence of a pentanol-2-ol side chain attached to C-11 of the core skeleton. The planar structure of **1** was thus established and confirmed by heteronuclear multiple bond correlations (HMBCs) (Fig. 3) and X-ray crystallographic diffraction analysis (Fig. 4).

Compound **2** was isolated as a white amorphous powder and exhibited the same molecular formula as **1**, as determined by HR-ESI-MS analysis. Comparison of the ^{1}H and ^{13}C NMR spectral data between **2** and **1** indicated identical structures. Furthermore, comprehensive analyses of the ^{1}H-^{1}H COSY, HSQC, and HMBC data corroborated that **2** shared the same planar structure as **1**.

The absolute configurations of C-15 in **1** and **2** were elucidated using the modified Mosher's method [7]. The positive values of $\Delta\delta_{H(S-R)}$, representing the differences between the ^{1}H NMR chemical shifts of (*S*)-MTPA ester and (*R*)-MTPA ester derivatives at H-14, coupled with the negative values of $\Delta\delta_{H(S-R)}$ at H-16, corroborated the *S* configuration of C-15 in both **1** and **2** (Fig. 5, Fig. S13, and Fig. S22). Additionally, the absolute configurations of C-11 in **1** and **2** were determined as *R* and *S*, respectively, through a comparison of their experimental electronic circular dichroism (ECD) curves with those of corynechromones A and B [7]. The ECD spectrum of **1** exhibited positive cotton effects at 215, 241, and 334 nm and negative cotton effects at 229 and 307 nm, indicative of the *R* configuration for C-11. Conversely, **2** displayed negative cotton effects at 216 and 331 nm and a positive cotton effect at 305 nm, corresponding to the *S* configuration for C-11 [7] (Fig. 6A).

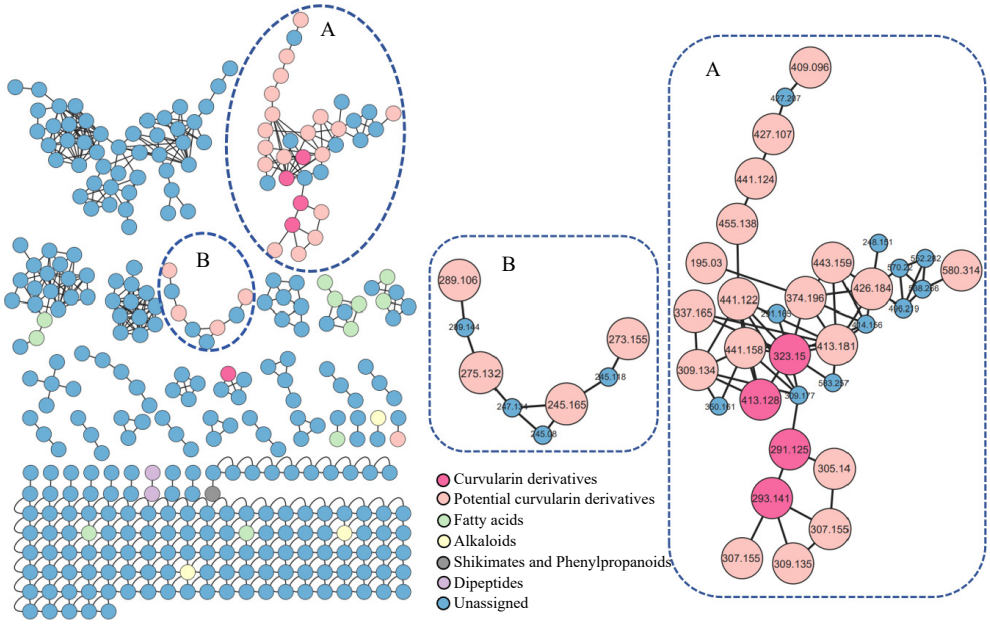

Fig. 1 Molecular networking for the extract of *Penicillium* sp. HL-50. Curvularin derivatives clusters correspond to proton adducts (A and B).

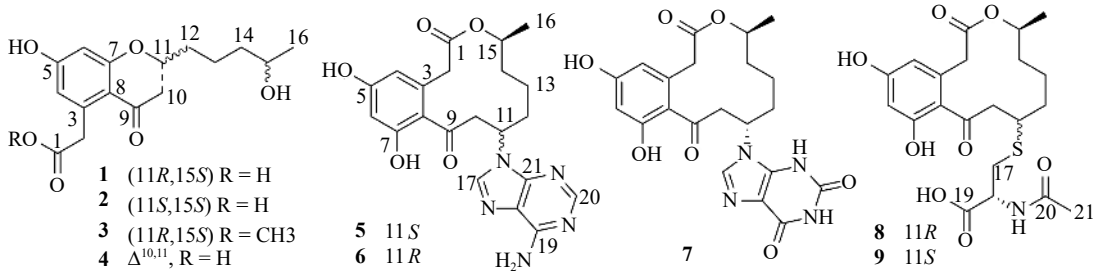

Fig. 2 Compounds **1**–**9** from *Penicillium* sp. HL-50.

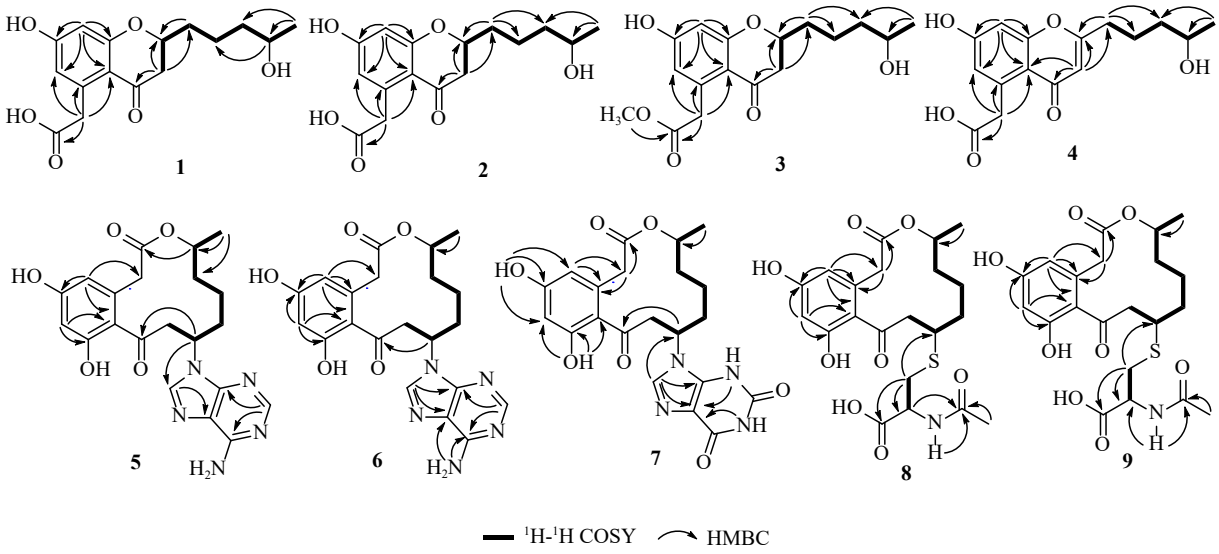

Fig. 3 The Key ^{1}H-^{1}H COSY and HMBCs of **1**–**9**.

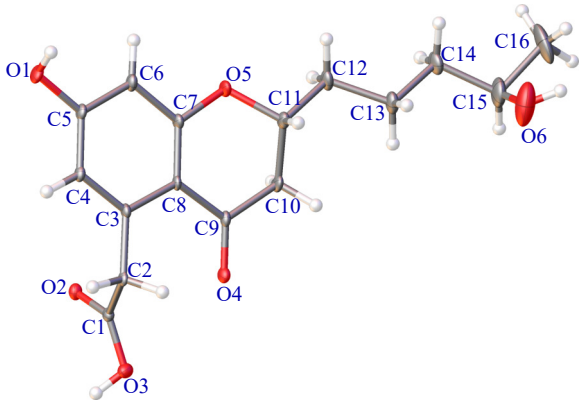

Fig. 4 X-ray crystallographic structure of **1**.

Consequently, the structures of compounds **1** and **2** were elucidated and designated as penicichromones A and B, respectively.

Compound **3** was isolated as a white amorphous powder, and its molecular formula was established as $C_{17}H_{22}O_6$ based on HR-ESI-MS data, indicating seven degrees of unsaturation. A comparison of the 1D NMR data with that of **1** (Table 1) revealed significant similarities, except for an additional methoxyl signal in **3** at δ_H 3.56 (3H, s) and δ_C 51.2. The HMBC of H-17 (δ_H 3.56) with C-1 (δ_C 171.0) assigned the methoxyl group to C-1, demonstrating that **3** was a methyl esterification derivative of **1**. The planar structure of **3** was thus determined and confirmed by ^{1}H-^{1}H COSY correlations and HMBCs (Fig. 3). As the experimental ECD curve of **3** was consistent with that of **1**, the absolute configuration of C-11 in **3** was deduced as *R* (Fig. 6A). The *S* configuration of C-15 in **3** was also determined using the modified Mosher's method (Fig. 5 and Fig. S31). Consequently, the structure of **3** was elucidated and designated as penicichromone C.

Compound **4** was isolated as a white amorphous powder. Its molecular formula was determined to be $C_{16}H_{18}O_6$ based on HR-ESI-MS analysis, indicating eight degrees of unsaturation, one more than that of **1**. A comparison of the 1D NMR data between **4** and **1** revealed significant similarities, with the main differences observed in the ^{1}H and ^{13}C resonances of C-10 and C-11. In **4**, an olefinic methylene at δ_H 5.94/δ_C 109.8 for C-10 and an olefinic quaternary carbon at δ_C 167.2 for C-11 were observed, in contrast to a methylene at δ_H 2.54/δ_C 43.3 for C-10 and a methine at δ_H 4.32/δ_C 76.8 for C-11 in **1**, indicating the presence of a double bond at C-10 and C-11 in **4**. The planar structure of **4** was elucidated and confirmed through analysis of its ^{1}H-^{1}H COSY, HSQC, and HMBC spectra. Due to the limited quantity of the compound, the absolute configuration of C-15 in **4** could not be determined using Mosher's method. The compound was subsequently named penicichromone D.

Compound **5** was isolated as a light yellow oil with a molecular formula of $C_{21}H_{23}N_5O_5$, indicating thirteen degrees of unsaturation. The ^{1}H NMR analysis of **5** revealed the characteristic signals for four aromatic or olefinic protons at δ_H 8.29 (1H, s), 8.13 (1H, s), 6.31 (1H, d, *J* = 1.6 Hz) and 6.25 (1H, brs), two amide protons at δ_H 7.19 (2H, s), two methines at δ_H 4.96 (1H, m) and 4.78 (1H, m), and a methyl at δ_H 1.10 (3H, d, *J* = 6.0 Hz). The ^{13}C NMR combined with HSQC data indicated the presence of 21 carbon resonances, including two carbonyl groups at δ_C 170.2 and 202.4, 11 aromatic or olefinic carbons, two methines, five methylenes, and a methyl. Analysis of the ^{1}H and ^{13}C NMR data suggested a curvularin structure skeleton, corroborated by fragment ions at *m/z* 291.1250 [4]. Additionally, a fragment with $[C_5H_5N_5 + H]^+$ at

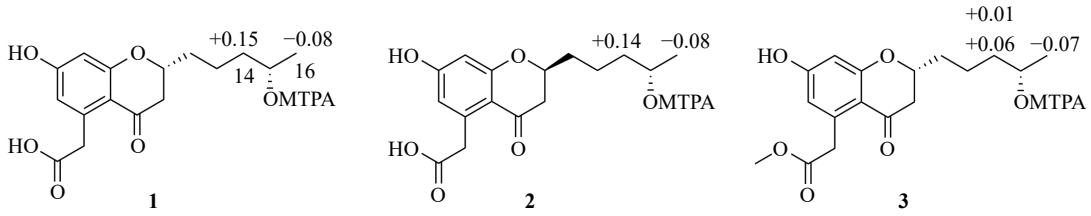

Fig. 5 Values of $\Delta\delta_{H(S-R)}$ of the MTPA esters of compounds **1**–**3**.

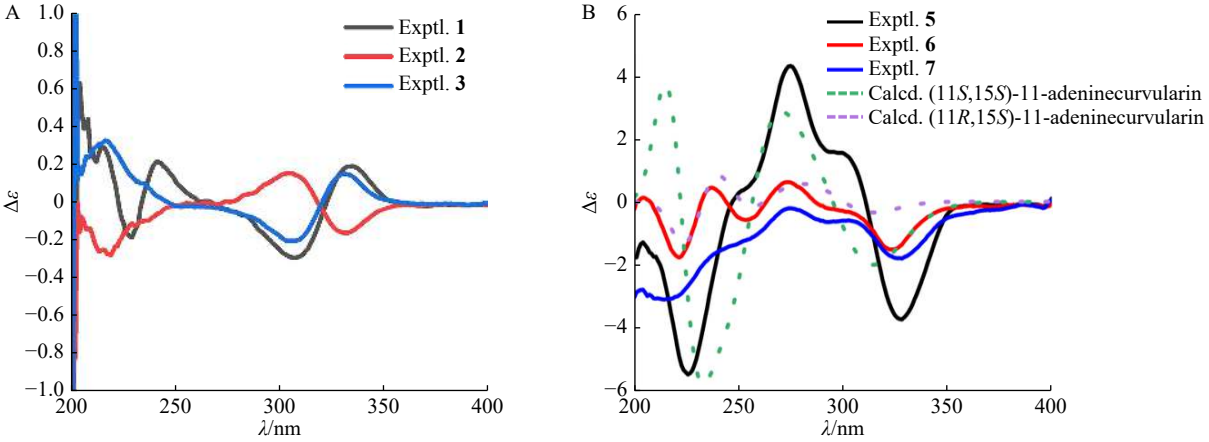

Fig. 6 ECD spectra of **1**–**3** and **5**–**7**. (A) Experimental ECD spectra of **1**–**3**; (B) Experimental and calculated ECD spectra of **5**–**7**.

m/z 136.0631 was identified as adenine by comparing the remaining NMR signals in **5** with those of adenine [21], supported by observed HMBCs from H-17 to C-18 and from H-20 to C-19 and C-21 (Fig. 3). The adenine moiety was determined to be attached to C-11 of **5** based on the HMBC from H-11 to C-17. The planar structure of **5** was thus elucidated and confirmed by key ^{1}H-^{1}H COSY correlations and HMBCs (Fig. 3).

Compound **6** was also isolated as a light yellow oil and exhibited the same molecular formula as **5**, as determined by HR-ESI-MS analysis. The striking similarities in the ^{1}H and ^{13}C NMR spectra of **6** and **5**, coupled with the key ^{1}H-^{1}H COSY correlations and HMBCs of **6** (Fig. 3), indicated that these compounds shared identical planar structures.

The structures of compounds **5** and **6** were further corroborated through chemical synthesis. Michael addition of (15*S*)-10,11-dehydrocurvularin (**11**) with adenine yielded compounds **5** and **6** under alkaline conditions (Fig. S2), indicating that **5** and **6** are epimers of C-11 with *S* configurations for C-15. The *S* and *R* configurations of C-11 for **5** and **6**, respectively, were determined by comparing the calculated ECD with their experimental CD spectra (Fig. 6B). Consequently, the structures of compounds **5** and **6** were elucidated and designated as (11*S*,15*S*)-11- and (11*R*,15*S*)-11-adeninecurvularin, respectively.

Compound **7** was isolated as a white amorphous powder with a molecular formula of $C_{21}H_{22}N_4O_7$. A comparison of the NMR data with that of **6** revealed they shared the same curvularin structure skeleton. The additional $C_5H_3N_4O_2$ unit in **7** was identified as xanthine by comparing its 1D NMR data with a previous report [22]. The HMBCs from H-17 to C-11, C-18, and C-21 and from NH to C-18 confirmed the presence of a xanthine moiety attached to the C-11 of the curvularin skeleton. The experimental ECD curve of **7** aligned well with that of **5**, in combination with their similar positive rotation values, indicating the C-11 configuration for **7** as *S* (Fig. 6B). Additionally, the absolute configuration of C-15 in **7** was determined to be consistent with that of **6** based on their common biosynthetic origins and comparison of their NMR data. Thus, the structure of **7** was elucidated and named (11*S*, 15*S*)-11-xanthinecurvularin.

Compounds **8** and **9** were isolated as colorless oils with the identical molecular formula $C_{21}H_{27}NO_8S$. Analysis of the ^{1}H and ^{13}C NMR data indicated that both were curvularin derivatives with identical planar structures. A comparison of the ^{1}H and ^{13}C NMR data of **8** and **9** with that of sumalarin C (**18**) revealed significant similarities, with the primary difference being additional acetyl signals [δ_H 1.86 (3H, s)/δ_C 22.5 and δ_C 169.5 for **8**; δ_H 1.85 (3H, s)/δ_C 22.4 and δ_C 169.2 for **9**] in **8** and **9**. Additionally, the ^{13}C resonance of C-18 shifted from δ_C 71.8 (sumalarin C, **18**) to δ_C 52.5 (**8**)/52.1 (**9**), indicating the replacement of the 18-OH in **18** with a *N*-acetyl group in **8** and **9**. The ^{1}H-^{1}H COSY correlations and HMBCs of **8** and **9** confirmed their identical planar structures. Michael additions of (15*S*)-10,11-dehydrocurvularin (**11**) with *N*-acetyl-L-cysteine produced compounds **8** and **9**, further confirming their structures (Fig. S3). The absolute configurations of C-15 and C-18 in **8** and **9** were determined to be *S*. Compounds **8** and **9** were identified as epimers of C-11. To determine the absolute configuration of C-11 in **8** and **9**, ^{13}C NMR calculation and $MAE_{\Delta\Delta\delta}$ value analysis were conducted [23]. The structures for 11*R* and 11*S* configurations were designated as **a** and **b**, respectively. Following conformational search and optimization, 5 stable conformers for **a** and 6 conformers for **b** were obtained for subsequent ^{13}C NMR calculation at the mPW1PW91/6-31 + G(d, p) level. The $MAE_{\Delta\Delta\delta}$ values of two possible experimental/calculated comparison alignments, calc_**a** calc_**b**/exp_**8** exp_**9** and calc_**a** calc_**b**/exp_**9** exp_**8**, were calculated as 1.68 and 2.81, respectively. As calc_**a** calc_**b**/exp_**8** exp_**9** exhibited a lower $MAE_{\Delta\Delta\delta}$ value, the absolute configurations for C-11 in **8** and **9** were determined as *R* and *S*, respectively (Table S3). Thus, the structures of compounds **8** and **9** were identified and named as (11*R*,15*S*)- and (11*S*,15*S*)-11-(*N*-acetyl-L-cysteine)-curvularin, respectively.

The anti-inflammatory bioactivities of the isolated compounds were evaluated by assessing NO release and the expression level of key regulatory proteins of inflammation in LPS-mediated murine macrophage RAW264.7 cells. The results indicated that compounds **5**–**9**, **11**, **12**, **14**–**16**, **18**, **19**, **21**, and **23**–**25** exhibited significant inhibitory effects on NO production in LPS-mediated macrophage RAW264.7 cells at 10 μmol·L^{-1}, with com-

Table 1 ^{1}H and ^{13}C NMR spectroscopic data for compounds **1**–**4**.

No.	**1**[a]		**2**[a]		**3**[b]		**4**[a]	
	δ_C	δ_H (J in Hz)	δ_C	δ_H (J in Hz)	δ_C	δ_H (J in Hz)	δ_C	δ_H (J in Hz)
1	173.4		172.2		171.0		172.5	
2	41.5	3.78, s	40.8	3.79, s	40.3	3.83, s	40.5	4.00, s
3	140.0		139.7		138.5		138.2	
4	114.2	6.30, brs	114.2	6.28, d, 2.0	114.5	6.29, brs	118.0	6.64, d, 1.6
5	163.4		163.0		163.5		161.4	
6	101.5	6.21, brs	101.8	6.23, d, 2.4	102.0	6.24, brs	101.4	6.70, brs
7	164.0		164.1		164.2		159.0	
8	112.0		112.2		111.7		114.2	
9	191.2		191.3		191.3		177.9	
10	43.3	2.54, m	43.2	2.56, dd, 16.8,12.0; 2.48,dd, 12.0, 4.8	43.0	2.56, dd, 16.4, 12.0 2.37, m	109.8	5.94, s
11	76.8	4.32, m	76.9	4.34, m	76.9	4.34, m	167.2	
12	34.2	1.56, m； 1.73, m	34.1	1.74, m; 1.62, m	34.1	1.70, m; 1.61,m	32.8	2.54, td, 7.2, 3.2
13	20.8	1.35, m; 1.58, m	20.9	1.58, m; 1.45, m	20.8	1.54, m; 1.45, m	22.7	1.73, m ;1.62, m
14	38.8	1.35, m	38.8	1.34, m	38.7	1.36, m;	38.1	1.37, m
15	65.6	3.58, m	65.7	3.59, m	65.6	3.58, m	65.4	3.62, m
16	23.7	1.05, d, 6.0	23.7	1.04, d, 6.4	23.7	1.04, d, 6.0	23.7	1.04, d, 6.0
17					51.2	3.56, s		

[a] Measured in DMSO-d_6 at 400 and 100 MHz for ^{1}H and ^{13}C, respectively; [b] measured in DMSO-d_6 at 400 and 150 MHz for ^{1}H and ^{13}C, respectively.

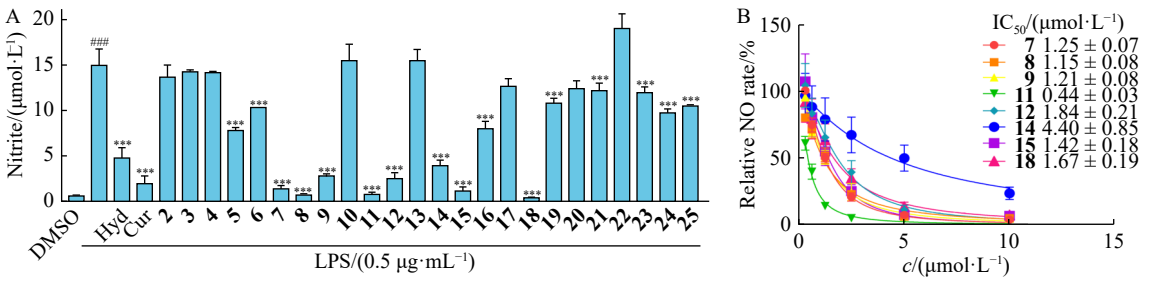

Fig. 7 Inhibitory effects of isolated compounds on NO production in LPS-stimulated RAW264.7 cells. Cells were treated with DMSO, 0.5 μg·mL^{-1} LPS, and the combination of 0.5 μg·mL^{-1} LPS with positive controls (Hyd and Cur) or compounds **2**–**25** at 10 μmol·L^{-1} (A) or specified concentrations of compounds **7**–**9**, **11**, **12**, **14**, **15**, and **18** (B) for 24 h. Subsequently, the release of NO in the culture media was measured using an NO assay kit. Data are presented as mean ± SD for (A) and mean ± SEM for (B) from three replications. $^{###}P < 0.001$ *vs* DMSO; $^{***}P < 0.001$ *vs* LPS.

pounds **7**–**9**, **11**, **12**, **14**, **15**, and **18** demonstrating inhibitory rates exceeding 50% (Fig. 7A). Concurrently, the cell survival assay revealed that compounds **3**–**5**, **11**, **15**, and **22** exhibited varying degrees of cytotoxicity towards RAW264.7 cells, while the other compounds did not display significant cytotoxicity at 10 μmol·L^{-1} (Fig. S1). Dose-dependent studies demonstrated that compounds **7**–**9**, **11**, **12**, **14**, **15**, and **18** significantly inhibited NO production in LPS-mediated RAW264.7 cells with IC_{50} values ranging from 0.44 to 4.40 μmol·L^{-1} (Fig. 7B). Structure-activity relationship (SAR) analysis indicated that curvularin derivatives with a benzene ring fused twelve-membered macrocyclic lactone skeleton exhibited stronger inhibitory activities compared to those with a fused six-membered cyclic ether skeleton (**1**–**4**) and the ring-opening curvularin derivatives (**21** and **22**). Furthermore, 10,11-dehydrocurvularin (**11**) and curvularin derivatives with C-11 substituents (**7**–**9**, **12**, **14**, **15**, and **18**) demonstrated enhanced inhibitory effects on NO production, suggesting the favorable role of *α*,*β*-unsaturated ketone in their anti-inflammatory activity. This is likely due to the potential transformation of C-11 substituted derivatives to yield 10,11-dehydrocurvularin (**11**). Our study highlighted the critical role of the 12-membered lactone ring in the anti-inflammatory potential of curvularin derivatives. Additionally, we confirmed the advantage of *α*,*β*- unsaturated ketone fragments for the anti-inflammatory activity of curvularin derivatives [13].

Furthermore, we assessed the inhibitory effects of the bioactive compounds **7**–**9**, **11**, **12**, **14**, **15**, and **18** on the expression levels of inflammation regulatory proteins, including iNOS, COX-2, NLRP3, and NF-*κ*B, in LPS-stimulated murine macrophage RAW264.7 cells. The results indicated that all compounds exhibited varying degrees of inhibition on the expression of these proteins. Notably, compounds **7** and **11** demonstrated superior inhibitory effects on NO production and the expression of inflammation regulatory proteins in LPS-stimulated RAW264.7 cells. In conclusion, this study provides evidence that curvularin derivatives exhibit potent anti-inflammatory properties, potentially involving multiple signaling pathways.

Subsequently, we investigated the anti-inflammatory proper-

ties of the novel compound **7**, which exhibited comparable anti-inflammatory activity to 10,11-dehydrocurvularin (**11**) but with reduced cytotoxicity. Our study demonstrated that compound **7** suppressed the expression of iNOS, COX-2, NLRP3, and pP65 in a dose-dependent manner (Fig. 8B and 8G–8J). Furthermore, we examined the inhibitory effects of **7** on the transcription of inflammation-related genes stimulated by LPS in RAW264.7 cells using quantitatieve polymerase chain reaction (qPCR). The results indicated that LPS significantly increased the mRNA levels of all tested genes except *Casp1*. Compound **7** was found to inhibit the LPS-induced transcriptional increase of inflammation-related genes, including *Nlrp3*, *Nos2* (encoding iNOS), *Nfκb1*, *Tnfα*, *Il-6*, *Il-1β*, and *Il-18*, in a concentration-dependent manner (Fig. 9).

In conclusion, this study identified nine novel curvularin derivatives (**1**–**9**) and 16 known analogs (**10**–**25**) from the hydrothermal vent sediment fungus *Penicillium* sp. HL-50 using molecular networking-guided targeted isolation. Notably, compounds **5**–**7** were curvularin derivatives containing a purine moiety, readily identified through MS/MS analysis. Naturally occurring curvularin derivatives primarily consist of a benzene ring fused to a twelve-membered macrocyclic lactone skeleton, typically with substituents at C-11. The planar structure of these compounds was characterized by the diagnostic ion of *m/z* 291 and the neutral loss of C-11 substituents. These findings demonstrate that liquid chromatography-tandem mass spectrometry (LC-MS/MS)-based molecular networking is an efficient strategy for accelerating the identification of bioactive and structurally novel components from marine fungi.

Pharmacological investigations revealed that curvularin derivatives, characterized by a benzene ring fused to a twelve-membered macrocyclic lactone core structure, particularly compounds **7**–**9**, **11**, **12**, **14**, **15**, and **18**, significantly inhibited LPS-induced NO production in RAW264.7 cells. Further analyses demonstrated their ability to downregulate inflammation-related proteins, including iNOS, COX-2, NLRP3, and pP65, with compounds **7** and **11** exhibiting more potent anti-inflammatory effects. Moreover, the novel compound **7** was shown to exert its anti-inflammatory function by suppressing the transcription of inflammation-related genes, reducing the expression of inflammation-related proteins, and inhibiting the release of inflammatory cytokines. While numerous studies have highlighted the anti-inflammatory potential of dehydrocurvularin (**11**), its cytotoxicity warrants consideration. Consequently, when developing this class of compounds as novel anti-inflammatory agents, careful attention must be given to their potential side effects.

In conclusion, this study enhances the structural diversity of curvularin derivatives while simultaneously investigating their structure-activity relationship and the underlying mechanisms of their anti-inflammatory effects.

3. Experimental

3.1. General experimental procedures

Chiroptical measurements were obtained using a P-1020 digital polarimeter (JASCO International Co., Ltd., Tokyo, Japan). Ultraviolet/Visible spectroscopy (UV/VIS) spectra were recorded

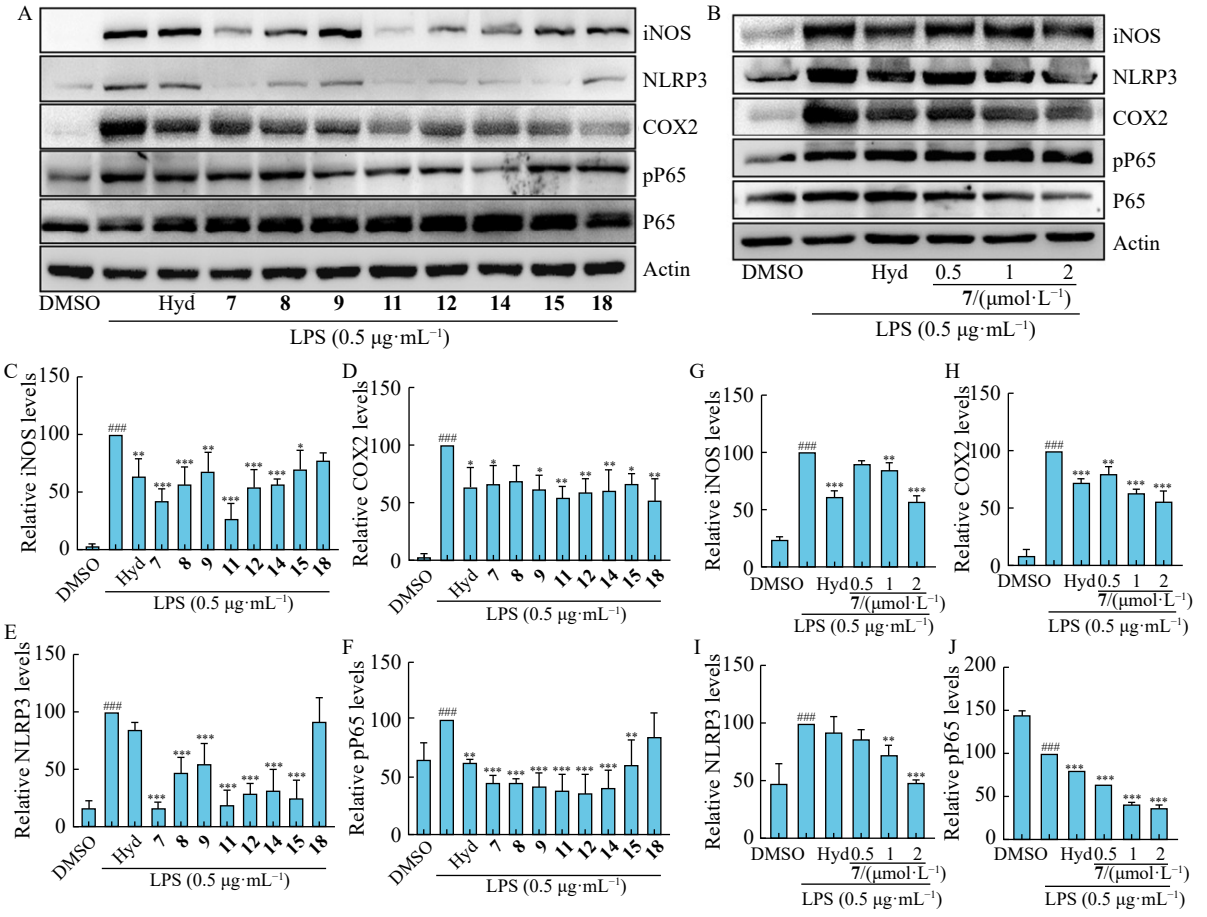

Fig. 8 Inhibitory effects of isolated compounds on key regulatory proteins of inflammation in LPS-induced RAW264.7 cells. Cells were treated with 0.5 μg·mL^{-1} LPS with or without 10 μmol·L^{-1} compounds **7**–**9**, **11**, **12**, **14**, **15**, and **18** (A) or varying concentrations of **7** (B) and incubated for 24 h. Subsequently, the expression levels of inflammatory regulatory proteins were assessed using Western blot assay. Quantification results of iNOS, COX-2, NLRP3, and pP65 (C–F) from (A) and (G–J) from (B) were obtained using ImageJ. Data are presented as mean ± SD from three replicates. $^{###}P < 0.001$ *vs* DMSO; $^{***}P < 0.001$, $^{**}P < 0.01$ and $^{*}P < 0.05$ *vs* LPS.

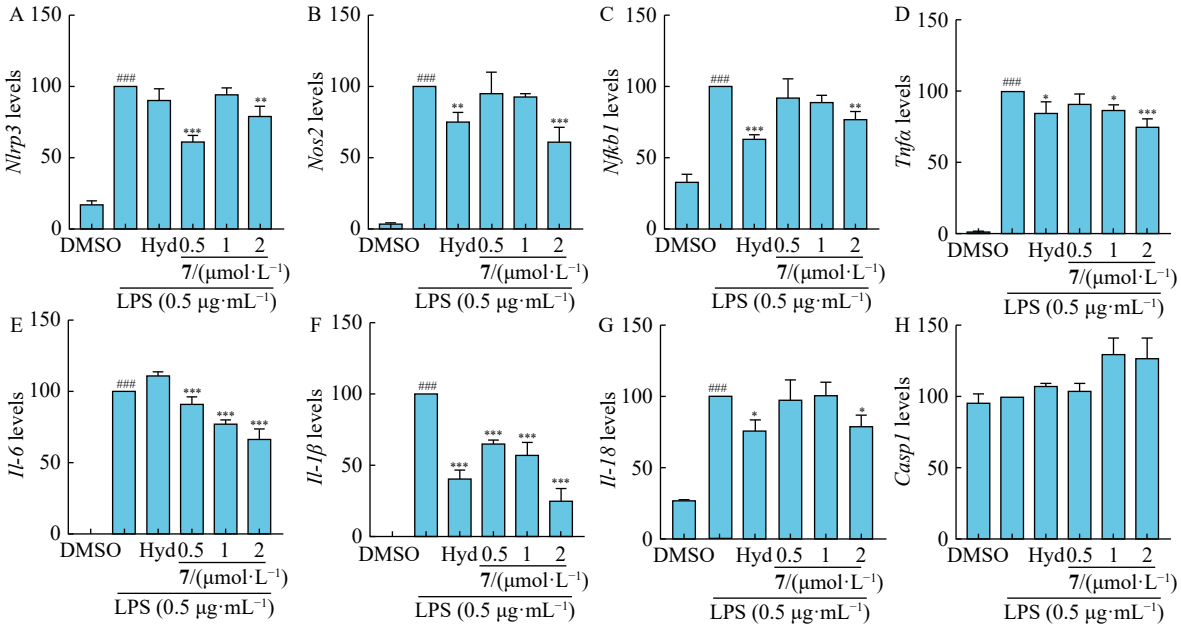

Fig. 9 Compound **7** inhibited inflammatory gene expressions at the mRNA level. RAW264.7 cells were treated with DMSO, 0.5 μg·mL^{-1} LPS, and the combination of hydrocortisone (Hyd) or compound **7** (0.5, 1, and 2 μmol·L^{-1}) with 0.5 μg·mL^{-1} LPS for 12 h. Subsequently, RNA was extracted, and the expression levels of genes including *Nlrp3* (A), *Nos2* (B), *Nfkb1* (C), *Tnfα* (D), *Il-6* (E), *Il-1β* (F), *Il-18* (G), and *Casp1* (H) were analyzed using qPCR. Data represent mean ± SD from three independent replicates. $^{###}P$ < 0.001 *vs*DMSO; $^{***}P$ < 0.001, $^{**}P$ < 0.01 and $^{*}P$ < 0.05 *vs* LPS.

on a JASCO V-550 UV/VIS spectrometer (JASCO, Tokyo, Japan), while CD spectra were acquired using a Chirascan Plus spectrometer (Applied Photo Physics Ltd., Leatherhead, UK). IR spectra were collected with a JASCO FT/IR-480 plus spectrometer (JASCO, Tokyo, Japan). HR-ESI-MS spectra were obtained using a Synapt G2 (Waters, Wilmslow, UK) mass spectrometer in positive ion mode. Column chromatography (CC) was performed using silica gel (200–300 mesh, Qingdao Marine Chemical Ltd., China) and ODS-A-HG (12 nm, YMC Co., Ltd., Japan). 1D and 2D NMR spectra were recorded on Bruker Avance 400 MHz and 600 MHz spectrometers with TMS as internal standard. Analytical and semi-preparative high-performance liquid chromatography (HPLC) were conducted on a Shimadzu LC-20AB system equipped with an LC-20AT pump, SIL-20A automated sample injector, and SPD-20A UV/VIS detector (Shimadzu, Tokyo, Japan). Columns for analytical and preparative HPLC were COSMOSIL Packed C_{18} columns (5 μm, ϕ 4.6 mm × 250 mm and 5 μm, ϕ 10 mm × 250 mm, respectively). MeOH and CH_3CN of HPLC grade were purchased from Thermo Fisher (Waltham, MA, USA). Analytical-grade solvents were used for solvent extractions, while HPLC-grade solvents from Thermo Fisher (Waltham, MA, USA) were employed for HPLC and LC-MS analyses, filtered and degassed through a 0.45 μm polytetrafluoroethylene (PTFE) membrane before use.

Curcumin (#T1516) and hydrocortisone (#H80017) were obtained from TargetMol (Boston, MA, USA) and Beijing Jin Ming Biotechnology Co., Ltd. (Beijing, China), respectively. The NO assay kit (#S0021) was procured from Beyotime Inst Biotech (Shanghai, China). Antibodies for iNOS (#13120), COX-2 (#12282), pP65 (#3033), P65 (#8242), and NLRP3 (#15101) were sourced from Cell Signalling Technology (Beverly, MA, USA); *β*-actin (#GB15003) was acquired from Servicebio (Wuhan, China). The RNeasy plus kit (#74134) and cDNA synthesis kit (#K1622) were purchased from Qiagen (Germany Town, MD, USA) and Thermo Scientific (Franklin, MA, USA), respectively. qPCR primers [*Nlrp3*: 5′-AGGATCTCGCATTGGTTCTG-3′ (F), 5′-GTTGGTTTTGAGCACAGAGG-3′ (R); *Nos2*: 5′-AGCCTGTGAGACCTTTGATG-3′ (F), 5′-TCAGCCTCATGGTAAACACG-3′ (R); *Nfkb1*: 5′-ATGGCAGACGATGATCCCTAC-3′ (F), 5′-TGTTGACAGTGGTATTTCTGGTG-3′ (R); *Il-6*: 5′-CAAAGCCAGAGTCCTTCAGAG-3′ (F), 5′-GTCCTTAGCCACTCCTTCTG-3′ (R); *Il-1β*: 5′-TCCTGTGTAATGAAAGACGGC-3′ (F), 5′-ACTCCACTTTGCTCTTGACTTC-3′ (R); *Il-18*: 5′-GTTCACTCTCACTAACTTACATCAAAG-3′ (F), 5′-TCTATAAATCATGCAGCCTCGG-3′ (R); *Tnfα*: 5′-TCAATCTGCCCAAGTACTTAGAC-3′ (F), 5′-CCTGAGCCATAATCCCCTTTC-3′ (R), and *Casp 1*: 5′-CTTGGAGACATCCTGTCAGGG-3′ (F), 5′-AGTCACAAGACCAGGCATATTCT-3′ (R)] were obtained from Sangon Biotech Co,. Ltd. (Shanghai, China).

3.2. Sample preparation for UPLC/Q-TOF MS analysis and molecular networking construction

The extract was dissolved in MeOH and prepared to a concentration of 20 mg·mL^{-1}. Following centrifugation of the dissolved solution at 23 000 r·min^{-1} for 10 min, 2 μL of the supernatant aliquot was utilized for UPLC/Q-TOF MS analysis. The resulting raw mass data were converted to .mzML file format using msCovert software and processed using MZmine 2.53. Subsequently, the MS/MS data (.mgf) were exported and uploaded to the GNPS (https://gnps.ucsd.edu) online platform to generate classical molecular networks. The molecular networking was then visualized using Cytoscape 3.7.2. The GNPS analysis results are accessible at https://gnps.ucsd.edu/ProteoSAFe/status.jsp?task=e637fda500c54429a54ce13bc24b79e8 Detailed experimental parameters are provided in the Supporting Information.

3.3. Fungal material

The fungal strain HL-50 was isolated from hydrothermal vent sediments collected from Kueishantao, Taiwan Province, China. The 18s rDNA sequence region [1304 base pairs (bp), GenBank accession No. OR432231] of strain HL-50 was amplified using PCR. Based on morphological characteristics and 18s rDNA sequence analysis, which showed 99.77% similarity to *Penicillium* sp. according to the morphological characteristics and the 18s rDNA sequence, which is 99.77% similar to that of *Penicillium* sp. (MG547961.1), the strain was identified as *Penicillium* sp.. The strain is preserved at the Ocean College, Zhejiang University

(Zhejiang, China).

3.4. Fermentation, extraction, and isolation

The fungus *Penicillium* sp. HL-50 was isolated from a hydrothermal vent sediment in Taiwan Province, China. Fresh spores of *Penicillium* sp. HL-50 were grown on a Potato Dextrose Agar (PDA) medium at 28 °C for 3 d and subsequently inoculated into rice solid medium (100.0 g rice and 110 mL distilled water) for 45 d at room temperature. The fermented cultures were extracted thrice with EtOAc to yield an extract (60.0 g). This extract was fractionated by silica gel CC (ϕ 8.0 cm × 50.0 cm, 200–300 mesh, 400.0 g) using a petroleum ether (PE)–EtOAc and EtOAc–MeOH elution system, resulting in 9 fractions (fractions 1–9) based on thin layer chromatography (TLC) analysis. Fraction 7 (9.5 g) was further purified by reversed-phase CC using YMC GEL-18 with a MeOH–H_2O gradient (from 30∶70 to 100∶0) to yield 11 subfractions (fractions 7-1 to 7-11). Compound **10** (8.0 g) was the major component of fraction 7-7, comprising approximately 20% of the total crude extract. Fraction 7-8 (300.0 mg) was further purified by silica gel CC eluting with a PE–EtOAC gradient (from 10∶1 to 1∶1) and then by semipreparative HPLC (COSMOSIL ODS column, 10 μm; 10.0 mm × 250 mm; 4 mL·min^{-1}) to afford compounds **11** (5.0 mg, t_R = 15.4 min, 45% MeOH), **21** (15.0 mg, t_R = 15.6 min, 45% MeOH), **22** (10.0 mg, t_R = 21.9 min, 45% MeOH), and **23** (2.0 mg, t_R = 20.1 min, 30% MeOH). Fraction 8 (7.0 g) was subjected to ODS CC (MeOH–H_2O, 20∶80–100∶0), and 34 subfractions were preliminarily collected (fraction 8-1–fraction 8-34). Fraction 8-1 underwent semipreparative HPLC (25% MeOH–H_2O with 0.1% HCOOH, 4 mL·min^{-1}) to yield compounds **16** (7.0 mg, t_R = 25.1 min) and **17** (11.0 mg, t_R = 32.7 min). The sample of fraction 8-7 was subjected to semipreparative HPLC to yield fractions 8-7-1 to 8-7-4. Fraction 8-7-3 underwent further semipreparative HPLC (25% CH_3CN–H_2O with 0.1% HCOOH, 4 mL·min^{-1}) to obtain compounds **3** (2.0 mg, t_R = 16.3 min) and **19** (4.0 mg, t_R = 33.3 min). Compound **24** (7.0 mg, t_R = 17.7 min) was isolated from fraction 8-14 through semi-preparative HPLC (55% MeOH–H_2O with 0.1% HCOOH, 4 mL·min^{-1}). Fraction 9 (6.0 g) was applied to ODS CC (MeOH–H_2O, 80∶20–0∶100), and 22 subfractions were preliminarily collected (fraction 9-1–fraction 9-22). Fraction 9-10 (1.6 g) was fractionated by CC over silica gel using PE–EtOAc (from 40∶1 to 0∶1) to yield 34 subfractions (9-10-1 to 9-10-34). Purification of fraction 9-10-3 (70.0 mg) by semi-preparative HPLC (45% MeOH–H_2O with 0.1% HCOOH, 4 mL·min^{-1}) yielded compounds **12** (1.5 mg, t_R = 13.7 min) and **13** (1.5 mg, t_R = 20.6 min). Fraction 9-10-6 (50.0 mg) was also purified by semi-preparative HPLC (25% CH_3CN–H_2O with 0.1% HCOOH, 4 mL·min^{-1}) to obtain compounds **14** (5.0 mg, t_R = 26.2 min) and **15** (13.0 mg, t_R = 27.2 min). Fractions 9-10-25 and 9-10-28 were both subjected to semi-preparative HPLC (40% MeOH–H_2O with 0.1% HCOOH, 4 mL·min^{-1}) for purification. Compounds **4** (2.0 mg, t_R = 19.4 min), **7** (20.0 mg, t_R = 15.3 min), **8** (12.0 mg, t_R = 26.9 min), and **9** (3.0 mg, t_R = 41.0 min) were obtained from fraction 9-10-25, while compounds **5** (12.0 mg, t_R = 7.3 min), **6** (12.0 mg, t_R = 7.9 min), **20** (40.0 mg, t_R = 13.9 min), and **25** (3.0 mg, t_R = 13.2 min) were yielded from fraction 9-10-28. The unseparated portions of fractions 8 and 9 were combined and subjected to semi-preparative liquid chromatography (20% CH_3CN–H_2O with 0.1% HCOOH, 4 mL·min^{-1}), leading to the isolation of compounds **1** (7.0 mg, t_R = 16.1 min), **2** (10.0 mg, t_R = 16.2 min) and **18** (10.0 mg, t_R = 32.8 min).

Penicichromone A (**1**): colorless crystals; melting point 121.0–123.4 °C; $[\alpha]_D^{25}$ +35.8 (*c*, 0.1, MeOH); UV (MeOH) λ_{max} (log ε) 219 (3.5), 237 (3.3), 277 (3.3), and 316 (3.0) nm; IR (KBr) ν_{max} 3550, 3413, 1627, 1555, 1420, 1158, and 620 cm^{-1}; ECD (1.6 mmol·L^{-1}, MeOH) λ_{max} ($\Delta\varepsilon$) 215 (+0.29), 229 (−0.18), 241 (+0.22), 307 (−0.29), 334 (+0.20); ^{1}H and ^{13}C NMR spectral data, presented in Table 1; HR-ESI-MS *m/z* 309.1341 $[M + H]^+$ (Calcd. for $C_{16}H_{21}O_6$, 309.1338).

Penicichromone B (**2**): white amorphous powder; $[\alpha]_D^{25}$ +30.4 (*c*, 0.1, MeOH); UV (MeOH) λ_{max} (log ε) 219 (3.5), 237 (3.2), 277 (3.3), and 313 (2.9) nm; IR (KBr) ν_{max} 3418, 2926, 1638, 1560, 1423, 1156, and 625 cm^{-1}; ECD (1.6 mmol·L^{-1}, MeOH) λ_{max} ($\Delta\varepsilon$) 216 (−0.25), 305 (+0.16), 331 (−0.16) nm; ^{1}H and ^{13}C NMR spectral data, presented in Table 1; HR-ESI-MS *m/z* 309.1339 $[M + H]^+$ (Calcd. for $C_{16}H_{21}O_6$, 309.1338).

Penicichromone C (**3**): white amorphous powder; $[\alpha]_D^{25}$ +21.7 (*c*, 0.09, MeOH); UV (MeOH) λ_{max} (log ε) 219 (3.4), 237 (3.2), 277 (3.2), and 313 (2.9) nm; IR (KBr) ν_{max} 3313, 2928, 1643, 1592, 1552, 1440, 1156, and 560 cm^{-1}; ECD (1.6 mmol·L^{-1}, MeOH) λ_{max} ($\Delta\varepsilon$) 216 (+0.33), 306 (−0.20), 330 (+0.15) nm; ^{1}H and ^{13}C NMR spectral data, presented in Table 1; HR-ESI-MS *m/z* 323.1488 $[M + H]^+$ (Calcd. for $C_{17}H_{23}O_6$, 323.1495).

Penicichromone D (**4**): white amorphous powder; $[\alpha]_D^{25}$ +93.0 (*c*, 0.04, MeOH); UV (MeOH) λ_{max} (log ε) 216 (3.4), 250 (3.3), and 291 (3.2) nm; IR (KBr) ν_{max} 3415, 3244, 1630, 1557, 1428, 1135, and 620 cm^{-1}; ^{1}H and ^{13}C NMR spectral data, presented in Table 1; HR-ESI-MS *m/z* 307.1190 $[M + H]^+$ (Calcd. for $C_{16}H_{19}O_6$, 307.1182).

(11*S*,15*S*)-11-Adeninecurvularin (**5**): light yellow oil; $[\alpha]_D^{25}$ +66.0 (*c*, 0.04, MeOH); UV (MeOH) λ_{max} (log ε) 205 (3.6), 265 (3.3), and 309 (2.8) nm; IR (KBr) ν_{max} 3550, 3473, 3415, 1630, 1555, 1135, and 620 cm^{-1}; ECD (0.24 mmol·L^{-1}, MeOH) λ_{max} ($\Delta\varepsilon$) 229 (−5.41), 278 (+4.32), 329 (−3.72) nm; ^{1}H and ^{13}C NMR spectral data, presented in Table 2; HR-ESI-MS *m/z* 426.1799 $[M + H]^+$ (Calcd. for $C_{21}H_{24}N_5O_5$, 426.1777).

(11*R*,15*S*)-11-Adeninecurvularin (**6**): light yellow oil; $[\alpha]_D^{25}$ −53.0 (*c*, 0.04, MeOH); UV (MeOH) λ_{max} (log ε) 205 (3.5), 266 (3.3), and 307 (2.8) nm; IR (KBr) ν_{max} 3547, 3468, 3415, 1636, 1555, 1423, 1135, and 625 cm^{-1}; ECD (0.24 mmol·L^{-1}, MeOH) λ_{max} ($\Delta\varepsilon$) 209 (+0.18), 226 (−1.77), 241 (+0.45), 257 (−0.58), 277 (+0.63), 325 (−1.51) nm; ^{1}H and ^{13}C NMR spectral data, presented in Table 2; HR-ESI-MS *m/z* 426.1775 $[M + H]^+$ (Calcd. for $C_{21}H_{24}N_5O_5$, 426.1777).

(11*S*,15*S*)-11-Xanthinecurvularin (**7**): white amorphous powder; $[\alpha]_D^{25}$ +43.6 (*c*, 0.1, MeOH); UV(MeOH) λ_{max} (log ε) 205 (3.6), 272 (3.3), and 311 (2.8) nm; IR (KBr) ν_{max} 3552, 3473, 3418, 1631, 1555, 1420, 1135, and 623 cm^{-1}; ECD (0.23 mmol·L^{-1}, MeOH) λ_{max} ($\Delta\varepsilon$) 244 (−1.58), 277 (−0.21), 308 (−0.63), 329 (−1.79) nm; ^{1}H and ^{13}C NMR spectral data, presented in Table 2; HR-ESI-MS *m/z* 443.1572 $[M + H]^+$ (Calcd. for $C_{21}H_{23}N_4O_7$, 443.1567).

(11*R*,15*S*)-11-(*N*-Acetyl-L-cysteine)-curvularin (**8**): colorless oil; $[\alpha]_D^{25}$ +68.0 (*c*, 0.05, MeOH); UV (MeOH) λ_{max} (log ε) 204 (3.6), 275 (3.0), and 312 (2.9) nm; IR (KBr) ν_{max} 3547, 3471, 3415, 1636, 1557, 1428, 1133, and 623 cm^{-1}; ^{1}H and ^{13}C NMR spectral data, presented in Table 2; HR-ESI-MS *m/z* 454.1538 $[M + H]^+$ (Calcd. for $C_{21}H_{28}NO_8S$, 454.1536).

(11*S*,15*S*)-11-(*N*-Acetyl-L-cysteine)-curvularin (**9**): colorless oil; $[\alpha]_D^{25}$ +47.6 (*c*, 0.05, MeOH); UV (MeOH) λ_{max} (log ε) 203 (3.6), 276 (3.0), and 311 (2.9) nm; IR (KBr) ν_{max} 3552, 3473, 3415, 1630, 1555, 1420, 1133, and 620 cm^{-1}; ^{1}H and ^{13}C NMR spectral data, presented in Table 2; HR-ESI-MS *m/z* 454.1540 $[M + H]^+$ (Calcd. for $C_{21}H_{28}NO_8S$, 454.1536).

Crystal data of **1**: $C_{16}H_{20}O_6$•1.125 H_2O (M = 328.59 g·mol^{-1}): triclinic, space group P-1 (no. 2), a = 5.3039 (12) Å, b = 7.2068 (9) Å, c = 22.181 (4) Å, α = 91.105 (13), β = 91.119 (18), γ = 109.012 (17), V = 801.2 (3) Å^3, Z = 2, T = 149.99 (10) K, μ(Cu Kα) = 0.903 mm^{-1}, *Dcalc* = 1.362 g·cm^{-3}, 4386 reflections measured (3.986 ≤ 2Θ ≤ 133.19), 2798 unique (R_{int} = 0.1102, R_{sigma} = 0.1863) which were used in all calculations. The final R_1 was 0.1448 [I > 2σ(I)], and wR_2 was 0.4235 (all data). The crystal data were deposited in the Cambridge Crystallographic Data Centre with CCDC number 2294661, which is accessible free of charge at https://www.

Table 2 ^{1}H and ^{13}C NMR spectroscopic data for compounds **5**–**9**.

	5[a]		**6**[b]		**7**[c]		**8**[b]		**9**[b]	
	δ_C	δ_H (*J* in Hz)	δ_C	δ_H (*J* in Hz)	δ_C	δ_H (*J* in Hz)	δ_C	δ_H (*J* in Hz)	δ_C	δ_H (*J* in Hz)
1	170.2		169.6		171.0		169.7		170.3	
2	40.0	3.81, overlap; 3.49, overlap	40.1	3.87, d, 15.6; 3.68, d, 15.2	39.8	3.88, overlap; 3.79, overlap	40.4	4.02, d; 16.0; 3.54,,d, 16.4	39.7	3.78, overlap; 3.36, overlap
3	137.8		137.1		137.7		137.3		132.6	
4	111.3	6.25, brs	111.4	6.22, brs	112.5	6.37, d, 2.4	111.9	6.18, d, 2.0	111.2	6.18, brs
5	163.3		160.6		161.1		160.4		159.7	
6	101.8	6.31, d, 1.6	102.0	6.34, brs	102.9	6.42 , d, 2.4	102.0	6.32, d, 2.0	101.8	6.28, brs
7	160.1		159.6		159.1		159.6		159.1	
8	117.7		117.4		120.0		117.7		118.1	
9	202.4		201.1		202.7		201.8		203.3	
10	49.7	3.83, m; 3.37, m	49.3	3.80, brd, 12.8; 3.27, brd, 14.4	51.0	3.68, m	49.4	3.31, m ; 3.06, m	48.6	3.17, m
11	50.0	4.96, m	50.2	4.97, m	54.5	5.20, m	40.7	3.27, m	39.5	3.16, m
12	31.9	1.93, m; 1.68,m	31.9	1.98, m; 1.86, m	33.2	2.08, m; 1.83, m	30.2	1.47, m; 1.38, m	32.8	1.43, m
13	22.0	1.33, m; 0.91, m	18.3	1.32, m; 1.06, m	22.8	1.39, m; 1.20, m	18.3	1.29, m; 1.22, m	20.0	1.17, m
14	30.8	1.68, m; 1.34, m	30.0	1.73, m; 1.31, m	32.3	1.74, m; 1.49, m	31.1	1.51, m; 1.35, m	33.4	1.41, m
15	72.6	4.78, m	70.2	4.97, m	73.3	4.85, m	69.4	4.86, m	72.3	4.74, m
16	21.2	1.10, d, 6.0	18.2	1.06, d, 6.4	21.5	1.14, d, 6.0	19.2	1.03, d, 6.0	21.0	1.08, d, 5.6
17	139.7	8.29, s	139.7	8.27, s	142.6	8.09, s	32.1	2.90, dd; 13.2, 5.2; 2.75, dd, 13.2, 5.2	31.6	2.92, dd, 13.6, 4.4; 2.76, dd, 13.2, 9.2
18	118.7		118.8		107.2		52.5	4.35, td, 8.0, 5.2	52.1	4.37, m
19	156.0		156.0		151.7		172.2		172.3	
20	152.3	8.13, s	152.3	8.11, s	156.1		169.5		169.2	
21	149.3		149.2		151.2		22.5	1.86, s	22.4	1.85, s
19-NH_2		7.19, s		7.18, s						
5-OH						9.02, s				
7-OH						9.38, s				
18-NH								8.21, d, 8.0		8.17, d, 6.4
19-NH						9.82, s				
20-NH						10.60, s				

[a] Measured in DMSO-d_6 at 400 and 100 MHz for ^{1}H and ^{13}C, respectively; [b] measured in DMSO-d_6 at 400 and 150 MHz for ^{1}H and ^{13}C, respectively; [c] measured in acetone-d_6 at 600 and 150 MHz for ^{1}H and ^{13}C, respectively.

ccdc.cam.ac.uk/structures/.

*3.5. Preparation of the (S)- and (R)-MTPA esters of **1**–**3***

The dried compound **1** (0.5 mg) was dissolved in 500 μL of pyridine-d_5 in the NMR tube. Subsequently, (*R*)-MTPA-Cl (8 μL) was added and thoroughly mixed to produce the (*S*)-MTPA ester **1s**. Treatment of **1** (0.5 mg) with (*S*)-MTPA-Cl (8 μL), following the aforementioned procedure, yielded the (*R*)-MTPA ester **1r**. The (*S*)-MTPA esters (**2s** and **3s**) and (*R*)-MTPA esters (**2r** and **3r**) were obtained using the same process employed for the preparation of **1s** and **1r**.

*3.6. Quantum chemical ECD calculations of **5**–**7***

Random conformational searches for (11*S*,15*S*)-11-adenine-curvularin and (11*R*,15*S*)-11-adeninecurvularin were conducted using the SYBYL X 2.1.1 program with the MMFF94s molecular force field. The resulting stable conformers were optimized using Gaussian09 software at the B3LYP/6-31G(d) level in the gas phase. These optimized stable conformers were then subjected to further ECD calculations at the cam-B3LYP/6-31 + G(d) level in methanol. The overall ECD data were weighted by Boltzmann distribution, and the ECD curves were generated using SpecDis 1.70.1 software [sigma/gamma = 0.3, UV correction = 10 or 20 nm for (11*S*,15*S*)-11-adeninecurvularin or (11*R*,15*S*)-11-adeninecurvularin, respectively].

*3.7. Quantum chemical NMR calculations of **8** and **9***

The initial 3D conformations of two plausible stereoisomers, **a** [(11*R*,15*S*)-11-(*N*-acetyl-L-cysteine)-curvularin] and **b** [(11*S*, 15*S*)-11-(*N*-acetyl-L-cysteine)-curvularin], of compounds **8** and **9** were generated using CORINA version 3.4. Conformer databases were then created in CONFLEX version 7.0 utilizing the MMFF94s force field. All acceptable conformers were optimized using the HF/6-31G(d) method in Gaussian 16, followed by further optimization at the cam-B3LYP/6-31G(d) level to determine the dihed-

ral angles. The optimized stable conformers of the two plausible stereoisomers were then employed for NMR calculations at the mPW1PW91/6-31 + G(d, p) level. Solvent effects were accounted for using the IEFPCM solvent model, with methanol as the solvent. The calculated NMR data were analyzed using the $MAE_{\Delta\Delta\delta}$ method to determine the absolute configurations of C-11 in compounds **8** and **9**.

3.8. Bioassays

The evaluation procedures for the anti-inflammatory activity of isolated compounds were consistent with our previous reports [24]. RAW264.7 cell line (American Type Culture Collection, ATCC) was cultured in Dulbecco's modified Eagle's medium containing 10% fetal bovine serum (ExCell bio) in an incubator with 98% humidity and 5% CO_2. The MTT assay was conducted to assess the cell viability of RAW264.7 cells treated with the tested compounds. Concurrently, the NO concentration was measured according to the protocol of the NO assay kit. Additionally, RAW264.7 cells cultured in six-well plates were treated with compounds and/or LPS (0.5 μg·mL^{-1}) for 24 h. Subsequently, the cells were harvested to analyze the expression levels of inflammation-related proteins, including iNOS, NLRP3, COX2, and pP65 by Western blot assay. Furthermore, after 12 h treatment with **7** (0.5, 1, and 5 μmol·L^{-1}) and/or LPS (0.5 μg·mL^{-1}), total cellular RNA was extracted from RAW264.7 cells using the Qiagen RNeasy plus kit to quantify the mRNA levels of inflammatory response genes, *Nlrp3*, *Nos2*, *Nfκb1*, *Tnfα*, *Il-6*, *Il-1β*, *Il-18*, and *Casp 1* by qPCR. The detailed procedure is provided in the Supporting Information.

3.9. Statistical analysis

The data were analyzed and processed using GraphPad Prism 8.0 software. Each assay was performed independently at least three times.

Funding

This research was funded by the National Key Research and Development Program of China (No. 2022YFC2804101), the Guangdong Provincial Key R&D Program (No. 2023B1111050011), the Guangdong Basic and Applied Basic Research Foundation (No. 2023A1515010432), the Guangzhou Basic and Applied Basic Research Foundation (No. 202201010305), and the High-Level Talents Special Program of Zhejiang (No. 2022R52036).

Declaration of competing interest

These authors have no conflict of interest to declare.

References

1 Musgrave OC. Curvularin. Part I. Isolation and partial characterisatioiz of a metabolic prodzcct from a new species of *Curvularia*. *J Chem Soc*. 1956;1956:4301–4305. https://doi.org/10.1039/JR9560004301.
2 Kusano M, Nakagami K, Fujioka S, et al. *β,γ*-Dehydrocurvularin and related compounds as nematicides of *Pratylenchus penetrans* from the fungus *Aspergillus* sp.. *Biosci Biotech Bioch*. 2003;67(6):1413–1416. https://doi.org/10.1271/bbb.67.1413.
3 Liu GR, Niu SB, Liu L, et al. Alterchromanone A, one new chromanone derivative from the mangrove endophytic fungus *Alternaria longipes*. *J Antibiot*. 2021;74(2):152–155. https://doi.org/10.1038/s41429-020-00364-4.
4 Meng LH, Li XM, Lv CT, et al. Sulfur-containing cytotoxic curvularin macrolides from *Penicillium sumatrense* MA-92, a fungus obtained from the rhizosphere of the mangrove *Lumnitzera racemosa*. *J Nat Prod*. 2013;76(11):2145–2149. https://doi.org/10.1021/np400614f.
5 Aly AH, Debbab A, Clements C, et al. NF kappa B inhibitors and antitrypanosomal metabolites from endophytic fungus *Penicillium* sp. isolated from *Limonium tubiflorum*. *Bioorgan Med Chem*. 2011;19(1):414–421. https://doi.org/10.1016/j.bmc.2010.11.012.
6 Liang QR, Sun YQ, Yu BX, et al. First total syntheses and spectral data corrections of 11-*β*-methoxycurvularin and 11-*α*-methoxycurvularin. *J Org Chem*. 2007;72(25):9846–9849. https://doi.org/10.1021/jo701885n.
7 Zhao DL, Shao CL, Gan LS, et al. Chromone derivatives from a sponge-derived strain of the fungus *Corynespora cassiicola*. *J Nat Prod*. 2015;78(2):286–293. https://doi.org/10.1021/np5009152.
8 Krohn K, Michel A, Bahramsari R, et al. Biologically active metabolites from fungi. Part 7. Aposhaerin A and B; two new chroman-4-ones from *Aposphaeria* sp.. *Nat Prod Lett*. 1996;8(1):43–48. https://doi.org/10.1080/10575639608043238.
9 Robeson DJ, Strobel GA, Strange RN. The identification of a major phytotoxic component from alternaria macrospora as *α,β*-dehydrocurvularin. *J Nat Prod*. 1985;48(1):139–141. https://doi.org/10.1021/np50037a028.
10 Kobayashi A, Hino T, Yata S, et al. Unique spindle poisons, curvularin and its derivatives, isolated from *Penicillium* species. *Agric Biol Chem*. 1988;52(12):3119–3123. https://doi.org/10.1080/00021369.1988.10869190.
11 Zhao Q, Feng MY, Jin S, et al. 10,11-Dehydrocurvularin attenuates inflammation by suppressing NLRP3 inflammasome activation. *Chin J Nat Med*. 2023;21(3):163–171. https://doi.org/10.1016/S1875-5364(23)60418-2.
12 Xu YC, Wang LP, Zhu GL, et al. New phenylpyridone derivatives from the *Penicillium sumatrense* GZWMJZ-313, a fungal endophyte of *Garcinia multiflora*. *Chin Chem Lett*. 2019;30(2):431–434. https://doi.org/10.1016/j.cclet.2018.08.015.
13 Ha TM, Ko W, Lee SJ, et al. Anti-inflammatory effects of curvularin-type metabolites from a marine-derived fungal strain *Penicillium* sp. SF-5859 in lipopolysaccharide-induced RAW264.7 macrophages. *Mar Drugs*. 2017;15(9):282/1–282/12. https://doi.org/10.3390/md15090282.
14 Fox RAE, Evanno L, Poupon E, et al. Natural products targeting strategies involving molecular networking: different manners, one goal. *J Nat Rep*. 2019;36(7):960–980. https://doi.org/10.1039/C9NP00006B.
15 Jarmusch SA, Van der Hooft JJJ, Dorrestein PC. et al. Advancements in capturing and mining mass spectrometry data are transforming natural products research. *J Nat Rep*. 2021;36(7):2066–2082. https://doi.org/10.1039/d1np00040c.
16 Witte TE, Villenueve N, Shields SW, et al. Untargeted metabolomics screening reveals unique secondary metabolite production from *Alternaria* section *Alternaria*. *Front Mol Biosci*. 2022;9:1038299. https://doi.org/10.3389/fmolb.2022.1038299.
17 Augusto LS, Marisa I, Renato H, et al. Molecular network for accessing polyketide derivatives from *Phomopsis* sp., an endophytic fungus of *Casearia arborea* (Salicaceae). *Phytochen Lett*. 2021;42:1–7. https://doi.org/10.1016/j.phytol.2020.11.020.
18 Xu J, Kjer J, Sendker J, et al. Cytosporones, coumarins, and an alkaloid from the endophytic fungus *Pestalotiopsis* sp. isolated from the Chinese mangrove plant *Rhizophora mucronata*. *Bioorgan Med Chem*. 2009;17(20):7362–7367. https://doi.org/10.1016/j.bmc.2009.08.031.
19 Choochuay J, Xu X, Rukachaisirikul V, et al. Curvularin derivatives from the soil-derived fungus *Aspergillus polyporicola* PSU-RSPG187. *Phytochem Lett*. 2017;22:122–127. https://doi.org/10.1016/j.phytol.2017.09.011.
20 De Castro MV, Ioca LP, Williams DE, et al. Condensation of macrocyclic polyketides produced by *Penicillium* sp. DRF2 with mercaptopyruvate represents a new fungal detoxification pathway. *J Nat Prod*. 2016;79(6):1668–1678. https://doi.org/10.1021/acs.jnatprod.6b00295.
21 Zhou JL, Jiang Y, Bi ZM, et al. Study on nucleosides from *Fritillaria puqiensis*. *Chin Pharm J*. 2008;43(12):894–896.
22 Katarzyna D, Sergey M, Adam G. Structure of neutral molecules and monoanions of selected oxopurines in aqueous solutions as studied by NMR spectroscopy and theoretical calculations. *J Phys Chem A*. 2011;115(10):2057–2064. https://doi.org/10.1021/jp110888m.
23 Lauro G, Das P, Riccio R, et al. DFT/NMR approach for the configuration assignment of groups of stereoisomers by the combination and comparison of experimental and predicted sets of data. *J Org Chem*. 2020;85(5):3297–3306. https://doi.org/10.1021/acs.joc.9b03129.
24 Wang FF, Zhang M, Yuan M, et al. A novel sorbicillinoid compound as a potent anti-inflammation agent through inducing NLRP3 protein degradation. *Brit J Pharmacol*. 2023;180(15):1930–1948. https://doi.org/10.1111/bph.16058.